Journal of Engineering Science and Technology
Vol. 13, No. 9 (2018) 2700 - 2715

CHARACTERIZATION OF THE SONICATED YAM BEAN STARCH BIONANOCOMPOSITES REINFORCED BY NANOCELLULOSE WATER HYACINTH FIBER (WHF): THE EFFECT OF VARIOUS FIBER LOADING

MOCHAMAD ASROFI[1], HAIRUL ABRAL[1,*], ANWAR KASIM[2], ADJAR PRATOTO[1], MELBI MAHARDIKA[1], FADLI HAFIZULHAQ[1]

[1]Department of Mechanical Engineering, Andalas University, Kampus Limau Manis, Pauh, Padang 25163, Sumatera Barat, Indonesia
[2]Department of Agriculture Technology, Andalas University, Kampus Limau Manis, Pauh, Padang 25163, Sumatera Barat, Indonesia
*Corresponding Author: abral@ft.unand.ac.id

Abstract

Bionanocomposites based on a Yam Bean (Pachyrhizus spp.) (YB) starch matrix reinforced by nanocellulose Water Hyacinth Fiber (WHF) were produced using a casting method. The amount of nanocellulose suspension in the matrix was varied from 0 to 1 wt%. After gelation, the bionanocomposites were sonicated for 1 min. The effect of nanocellulose suspension loading on the YB starch matrix was analysed using tensile tests, Scanning Electron Microscopy (SEM), X-Ray Diffraction (XRD), Thermogravimetric Analysis (TGA), Fourier Transform Infrared (FTIR) and moisture absorption. The fracture surface of bionanocomposites is rougher than pure YB starch film. Tensile Strength (TS) and Tensile Modulus (TM) were significantly improved after addition of nanocellulose. The highest values for TS (5.8 MPa) and TM (403 MPa) were obtained using the highest proportion of nanocellulose (1 wt%). Crystallinity Index (*CrI*) of bionanocomposite increased more than 200% with additional nanocellulose just lower than 1 wt%. Thermal stability and moisture resistance were also raised with increasing nanocellulose loading. This bionanocomposite's mechanical and thermal properties suggest it could be suitable for food packaging.

Keywords: Bionanocomposites, Nanocellulose, Sonication, Water hyacinth fiber, Yam bean starch.

1. Introduction

In the last two decades, pollution due to plastics has become a serious problem on land, in rivers and also in the ocean. Many researchers have focused their attention on finding suitable biodegradable material to replace petroleum-based plastics that do not biodegrade and use non-renewable resources [1, 2]. Bioplastic, such as thermoplastic starch (TPS) is a good example of biodegradable material to replace non-biodegradable plastic [3, 4]. TPS is made by subjecting starch to high temperatures and shear forces and adding glycerol to reduce ductility [3]. However, pure TPS tends to be hydrophilic, have low mechanical, thermal, and water resistance properties. To overcome these disadvantages, natural fibers have been used as a reinforcement material for TPS [5].

Water Hyacinth Fiber (WHF) is one such potential natural fiber being cheap, nontoxic, and abundant in waterways in many tropical countries including Indonesia. Generally, WHF is considered a useless troublesome weed [6, 7]. However, this research is using WHF as reinforcing filler for TPS, providing an environmentally friendly plastic as reported in previous research [8, 9].

Much work is being done on natural fiber reinforced TPS. Sources of fibers that have been investigated include luffa [3], cassava bagasse [10], rice husks [11], Oil Palm Empty Fruit Bunch (OPEFB) [12], sugarcane bagasse [13], pineapple leaf fiber [14], and ramie [15]. All these produce fibers that have been shown to significantly improve the mechanical properties of a TPS matrix [2, 16]. However, micro-size fibers are not dispersed well in the TPS matrix, which results in agglomerations and porosities that are evident in SEM studies of fracture surfaces [17, 18]. If the fiber is broken down into nano-sized particles these problems can be effectively overcome as reported by a previous study [15, 19, 20].

Nanofibers have a larger contact surface area, lower density, higher thermal stability and better mechanical properties than micro-size fiber [21, 22]. It has been shown to be an effective filler in TPS matrix film resulting in films with high transparency, good mechanical and thermal properties [2, 17, 23]. The previous researcher reported a tensile test of a nanocomposite from the TPS matrix from corn starch with 5 wt% cotton cellulose nanofiber had 150% better TS compared to the pure TPS film. Thermal properties were also slightly improved [17]. The addition of nanocellulose fiber also increases water resistance as reported in previous research [5].

However, the dispersion of nanocellulose always a critical factor that highly influenced the mechanical strength of the TPS composite [17, 24, 25]. To overcome this issue, the sonication was used during the gelation formation. This is to ensure the homogeneous dispersion of nanocellulose, reduce porosity, and improve interfacial bonding between matrix and fiber [12, 18, 26].

Yam Bean (YB) tubers are commonly grown in a number of tropical countries and have a high starch content. This starch differs from those more commonly used in bioplastics as it has a particularly high amylopectin content, which generally has superior mechanical and thermal properties to amylose [27, 28].

There are many kinds of literature reported about natural fiber reinforced TPS composites. However, the study related nanocomposites made from WHF nanocellulose and YB starch based TPS matrix are not found in any literature. Hence, the effect of the addition of the nanocellulose WHF suspension to YB starch matrix composites was

investigated in the present research. Morphological, mechanical, thermal, crystallinity, functional group and moisture absorption properties were analysed.

2. Materials and Methods

2.1. Materials

Locally grown YB tubers were purchased in Padang, Indonesia. Starch was extracted from the tubers. The amylose and amylopectin content was measured to be 43% and 57%, respectively. Water hyacinth plants were obtained from a river in Payakumbuh, Indonesia and processed to extract the WHF as explained in section 2.3. Glycerin (Brataco brand)(density: 1.255-1.260 g/m*l*) was purchased from PT. Brataco, Padang. Other chemical reagents were supplied by the Mechanic and Metallurgy Laboratory, Andalas University.

2.2. Extraction of YB starch

YB tuber was cleaned and peeled, cut into small pieces and crushed by a "Slow Grinding Fruit Juicer" machine (model: SKG-J-1001). The bagasse of YB tubers and YB suspension were separated in the juicer machine. YB suspension was filtered through a 200 µm mesh sieve and then precipitated out and dried in a drying oven at 50 ^{o}C for 24 h. The YB starch was collected in the form of a powder.

2.3. Preparation of nanocellulose WHF

WHF was washed with distilled water and dried in the drying oven at 60 ^{o}C for 12 h until constant weight. After drying, it was cut into about 1 cm lengths with scissors. The dried WHF was immersed into a 15% sodium hydroxide solution and cooked in a digester (high-pressure reactor). Then, it was bleached by a solution of $NaClO_2$: CH_3COOH (in ratio 4:1). It was washed with distilled water until pH 7. The bleached WHF was treated again with 5 mol of the hydrochloric acid solution at 50 ^{o}C for 12 h to produce a cellulose suspension. This suspension was sonicated for 1 h (600 W) and maintained below 50 ^{o}C.

2.4. Fabrication of bionanocomposites

10 wt% YB starch, 2 m*l* glycerol, 100 m*l* distillate water and nanocellulose WHF suspension (0, 0.1, 0.3, 0.5, and 1 wt% from dry starch weight basis) were mixed in a glass beaker. The mixture was heated and stirred at 60 ^{o}C and 500 rpm for 30 min until gelatinized. Then, it was sonicated using an ultrasonic probe (SJIA-1200 W, diameter: 20 mm) for 1 min (600 W) at below 60 ^{o}C. The mixture was poured into a petri dish (diameter 15 cm) and dried in a drying oven at 50 ^{o}C for 20 h before characterization as suggested by a previous report [29].

3. Characterization of Bionanocomposites

3.1. Morphological surface investigation

The morphology of nanocellulose WHF was examined using a Transmission Electron Microscopy (TEM) JEM-JEOL 1400 instrument with an operation voltage of 100 keV. The fracture surface of bionanocomposite samples were observed using a SEM VEGA3 TESCAN with an operation voltage of 10 kV. Before testing, the SEM samples were coated with Palladium-Gold (Pd-Au).

3.2. Mechanical properties

All bionanocomposite samples were prepared and cut according to the ASTM D882-97 standard. Samples were prepared with five repeats for each concentration of WHF. The thickness and width of each sample were measured using a micrometer instrument (accuracy 0.001 mm) at five points for accuracy. Mechanical properties of bionanocomposite films were determined by the tensile test using COM-TEN 95T Series 5K (maximum capacity: 5000 pounds). The output of the tensile test was a tensile strength, tensile modulus, and elongation at break. Before testing, all bionanocomposite samples were conditioned at a relative humidity (RH) 55% in a desiccator for 2 days. Tensile tests were conducted at 25 ^{o}C and at 5 mm/min.

3.3. Thermal degradation

The thermal characteristics of 2.5 mg samples of YB starch film with and without WHF nanocellulose were investigated using a TGA/DTG-60 (Serial no. C30565000570) from 30-550 ^{o}C under a nitrogen atmosphere (flow rate: 50 m*l*/min). The heating rate was 20 ^{o}C/min.

3.4. Crystallinity index measurement

The XRD pattern of all studied samples was performed by using a PAN analytical Xpert PRO. The operation voltage and current were 40 kV and 35 mA, respectively. The diffraction intensity was recorded at (2θ= 10-40^{o}), (λ=0.154 nm). Segal et al. [30] determined Crystallinity index of the fiber as in Eq. (1):

$$C_rI = \left[\frac{I_{00\,2} - I_{am}}{I_{002}} \right] x\ 100\% \quad (1)$$

where, I_{002} maximum peak intensity at (2θ = 22.6^{o}) and I_{am} diffraction intensity at (2θ = 18^{o}). Meanwhile, the crystallinity index of YB starch and the bionanocomposite films according to V_H-type crystallinity, which calculated using the height ratio of diffraction peak (V_H-type at 2θ= 19.6^{o}) and B-type at 2θ= 16.8^{o}), as in previous reports [17, 31]. Hulleman et al. method [31] corresponds to the calculation of crystallinity as according to Eq. (2):

$$C_rI = \frac{H_c}{(H_c + H_a)}\ x\ 100\% \quad (2)$$

where H_c was the distance between the maximum peak at (2θ= 19.6^{o}) with its baseline. H_a was the distance between baseline H_c with its baseline at (2θ = 16.8^{o}).

3.5. Functional group determination

All film samples were cut into 1 cm ×1 cm squares and dried in drying oven at 50 ^{o}C overnight before characterization. The functional groups of all bionanocomposite samples were observed using FTIR mixed with KBr powder and pressed to become the transparent KBr-sample pellet. The spectrum was recorded using a Perkin-Elmer Frontier between wave numbers 600-4000 cm^{-1} under resolution 4 cm^{-1}.

3.6. Moisture absorption testing

All samples tested were cut 1.5 cm × 1 cm and dried until constant weight in a drying oven. Initial and final weight was (W_0) and (W_t), respectively. The moisture absorption

test was conducted in the moisture chamber (relative humidity 75% and temperature 25 ^{o}C) for 7 h. W_t of the sample was measured at 30 min intervals. The percentage moisture absorption of all tested samples was calculated according to Eq. (3) [12]:

$$\text{Moisture Absorption} = \left[\frac{W_t - W_0}{W_0}\right] \times 100\% \quad (3)$$

4. Results and Discussion

4.1. Morphological of nanocellulose

TEM images of nanocellulose WHF are displayed in Fig. 1. The fibers are short with diameter and length 15 and 150 nm, respectively. They appear to be distributed homogeneously due to probably the high-power intensity sonication. This result is similar to that previously reported for cassava bagasse cellulose nanofiber [10].

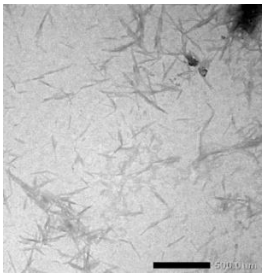

Fig. 1. TEM images of nanocellulose WHF.

4.2. Fracture surface of bionanocomposites

Figures 2(a) to (e) show the fracture morphology of all bionanocomposites using SEM. Pure YB starch film had a smooth surface and showed no aggregations (Fig. 2(a)). This indicates a good interaction between the YB starch and glycerol [11, 20]. The addition of nanocellulose suspension changes the morphology. As in previous studies, bionanocomposites have a rougher surface due to the presence of nanocellulose in the matrix. [11, 32]. It can be seen, the nanocellulose did not appear clearly. However, SEM is of limited use when used with nanosized fibers [2]. According to previous reports, SEM cannot be used to accurately determine the homogeneity of the dispersion of nanofiller throughout the matrix. [2, 20, 33]. This can be more easily inferred from the mechanical properties.

At the addition of 0.5 wt% of fiber, starch granules are visible in several places due to incomplete gelation of the starch during the fabrication process (see Fig. 2(d)). Similar insoluble starch has been reported in previous studies and has been found to decrease mechanical properties [34, 35]. The mobility of the nanocellulose polymer chain is obstructed within the starch matrix resulting in less effective reinforcing [12, 18, 26, 34].

Meanwhile, the bionanocomposites with 0.3 and 1 wt% WHF show beach mark fractures. According to previous reports, this is an indication of homogenous dispersion of nanocellulose and glycerol in the matrix and shows a good interaction between the hydroxyl groups of the matrix and the fiber [2, 22]. However, the presenting of nanocellulose in bionanocomposites gives brittle properties than YB starch film [5]. This phenomenon was supported by mechanical properties.

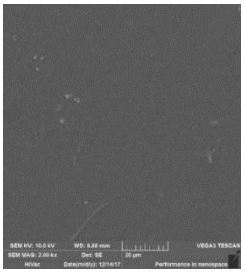

(a) 0 wt% nanocellulose in matrix.

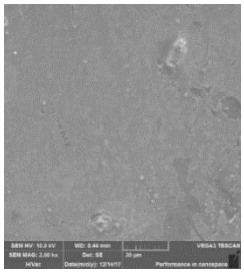

(b) 0.1 wt% nanocellulose in matrix.

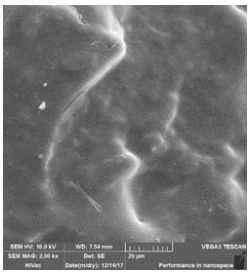

(c) 0.3 wt% nanocellulose in matrix.

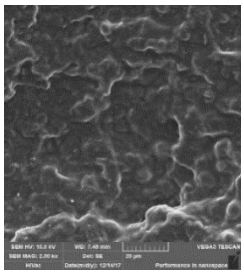

(d) 0.5 wt% nanocellulose in matrix.

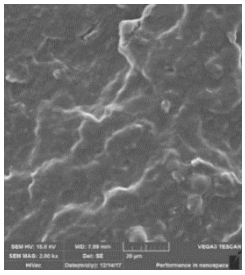

(e) 1 wt% nanocellulose in matrix.

Fig. 2. Fracture surface of all bionanocomposites by SEM.

4.3. Mechanical properties

Three aspects of the mechanical properties of the bionanocomposites were conducted; Tensile Strength (TS), Tensile Modulus (TM) and Elongation at Break (EB). The TS of bionanocomposites increased with the addition of nanocellulose (Fig. 3(a)). The addition of 0.1 wt% nanocellulose increased TS 80% compared to pure YB starch film and increased it to 360% and 480%, with the addition of 0.3 and 1 wt%, respectively. This pattern of increasing improvement is expected and probably indicates strong bonding between nanocellulose and the YB starch matrix [1, 11]. This result for nanocellulose WHF loaded YB starch film was better than that achieved by the previous report with nanocellulose cotton loaded corn starch TPS. The maximum TS for the latter was 0.35 MPa at 5 wt% compared to 5.8 MPa at 1 wt%. The addition of nanosized WHF improved TS of YB matrix by 400% compared to only 150% for cotton fiber loaded corn starch [17]. Biofilms reinforced with kenaf bast fiber nanocellulose had less than half the TS compared to the strongest bionanocomposites film in this present study [36].

In general, the higher loading of nanocellulose resulting in the higher value of TS except for the addition of 0.5 wt% of nanocellulose. This unexpected decrease

must be due to the presence of insoluble starch at several fracture points of the bionanocomposite due to poor mixing during fabrication leading to inferior incorporation of the nanocellulose into the YB starch matrix at these points [27]. This phenomenon was supported by SEM analysis (see Fig. 2(d)).

The addition of nanocellulose suspension also increased the TM of YB starch film. The TM with the addition of 1 wt% (Fig. 3(b)) was almost 8 times higher than of YB starch films. This was due to good nanocellulose dispersion as indicated by SEM and supported by previous reports [7, 23].

However, EB of YB starch film decreased with the increasing of nanocellulose suspension. Figure 3(c) shows EB of bionanocomposites with a different variation of addition nanocellulose. YB starch film had higher EB than bionanocomposites. This indicates that the bionanocomposite films are more brittle than untreated bionanocomposite films due to the decreasing mobility chain of starch [5].

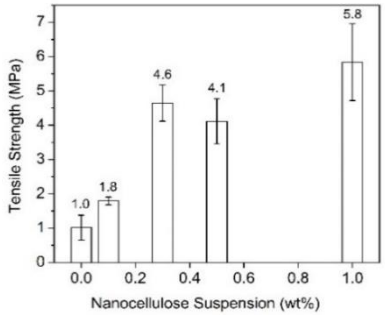

(a) Tensile strength.

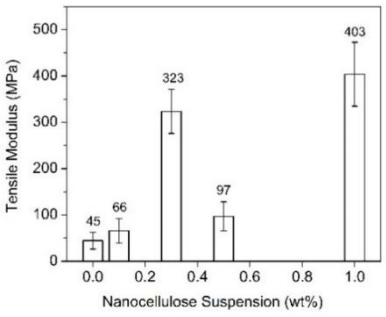

(b) Tensile modulus.

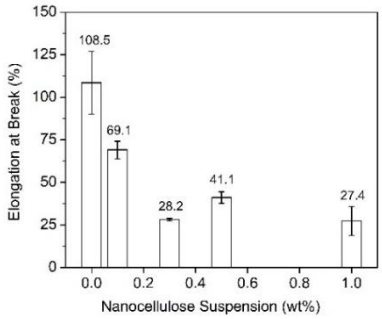

(c) Elongation at break.

Fig. 3. Mechanical properties of YB starch reinforced nanocellulose WHF based bionanocomposites.

4.4. Crystallinity index

Figure 4 presents the XRD diffraction pattern of nanocellulose WHF, YB starch film and bionanocomposites for 2θ=15-30°. The nanocellulose diffraction pattern (Fig. 4(a)) has two characteristic peaks at 2θ=22.6° and 18° corresponding to crystalline and amorphous structures, respectively. The crystallinity index is 82.5%. This result was higher than the previous one reported for nanocellulose garlic stalks [20].

The bionanocomposite films (Figs. 4(b) to (f)) have three main peaks [2, 13]. The characteristic peak at 2θ around 16.8° corresponds amylopectin recrystallization (B-type crystallization).

The intensity peak at 2θ around 19.6° corresponds to VH-type recrystallization of amylose during cooling after fabrication (retrogradation) because of the presence of lysophospholipids, isopropanol and glycerol. This result is expected having been observed in similar biocomposites [10, 17]. The peak at 2θ around 22.6° is due to the presence of nanocellulose WHF in YB starch film [13]. This peak did not appear in unreinforced YB starch film. The XRD patterns observed are similar to previous studies with other starch biocomposites [10].

Hulleman et al. [31] method was used for the crystallinity index for all bionanocomposite films' calculation as shown in Table 1. The nanocellulose in the YB starch matrix increased the crystallinity index of the bionanocomposites resulting in improved mechanical and thermal properties (see Figs. (3) and (5)).

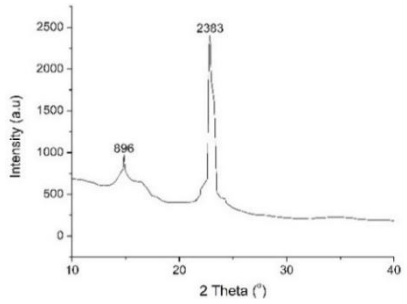

(a) Nanocellulose of WHF.

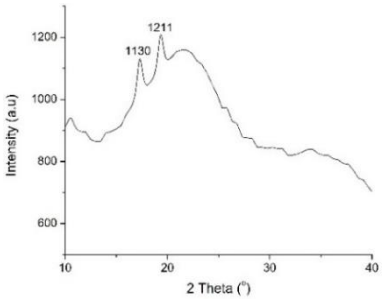

(b) Pure YB starch film.

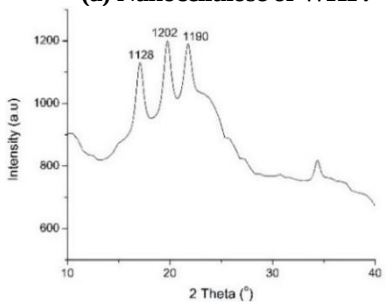

(c) 0.1 wt% nanocellulose in matrix.

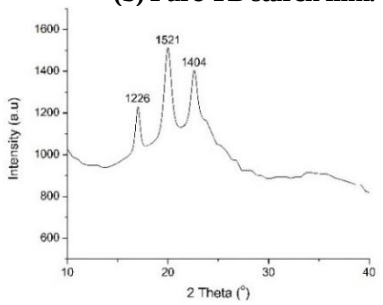

(d) 0.3 wt% nanocellulose in matrix.

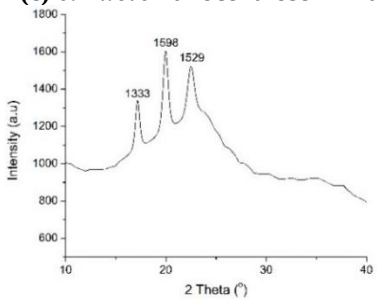

(e) 0.5 wt% nanocellulose in matrix.

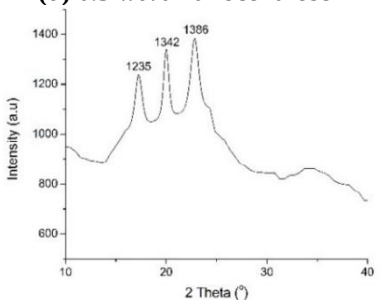

(f) 1 wt% nanocellulose in matrix.

Fig. 4. XRD pattern of all samples studied.

Table 1. Crystallinity index of all bionanocomposites samples.

Nanocellulose suspension (wt%)	H_c(a.u)	H_a(a.u)	C_rI(%)
0	10	262	23
0.1	182	198	48
0.3	380	193	66
0.5	372	249	60
1.0	284	163	64

4.5. Thermal stability

The thermogravimetric analysis (TGA) and differential thermal gravimetry (DTG) curve show the thermal characteristics of the bionanocomposites (Figs. 5(a) and (b)), respectively. As expected, there are three stages of degradation [37, 38]. All bionanocomposite films have higher thermal stability than YB starch film.

In the first region (60-140 ^oC) in Fig. 5(a) and Table 2, the major weight loss was due to moisture loss and was 12% in YB starch film; more than in any of the bionanocomposites due to the higher moisture content of the pure starch matrix [3, 39]. This phenomenon was agreement with the DTG curve (Fig. 5(b)) shows a small trough around 100 ^oC for the same reason.

All samples show major weight loss (up to 50%) in the second region between 210-350 ^oC as glycerol, starch and cellulose structure were all degraded. The onset temperature point of pure YB starch film was the lowest at 239 ^oC. This increased by 41, 51, 53, and 55 ^oC with addition of 0.1, 0.3, 0.5, 1 wt% nanocellulose, respectively (Table 2). At 1 wt% of nanocellulose in YB starch has higher onset temperature point than others nanocellulose loaded in bionanocomposite films, probably due to the good interaction of glycerol in the starch matrix and fiber [40, 41]. This result was agreement with SEM, XRD, and mechanical properties. The similar phenomenon was reported by the previous report for TPS from rice starch reinforced by cotton fiber [40].

However, this improved thermal stability with the addition of nanocellulose is expected and is a result of improved adhesion bonding with the YB starch matrix [17, 42]. The final weight loss occurred at over 350 ^oC, at which stage, all samples were perfectly decomposed to become CO_2 and volatile hydrocarbons [42, 43].

Table 2. Onset temperature of all bionanocomposites samples.

Nanocellulose suspension (wt%)	Temperature (^oC)		
	First region	Second region	Third region
0	92	239	341
0.1	95	280	363
0.3	96	290	365
0.5	106	292	368
1.0	111	294	371

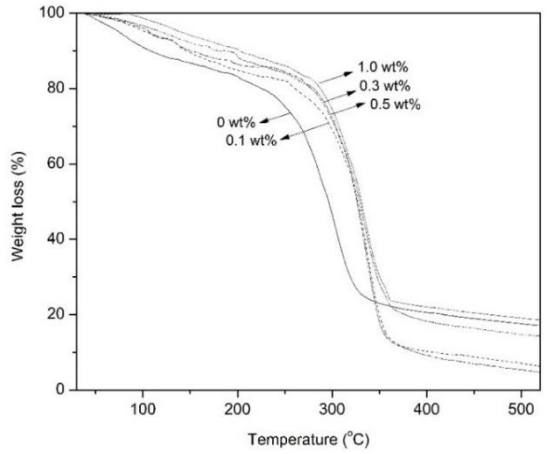

(a) TGA curve.

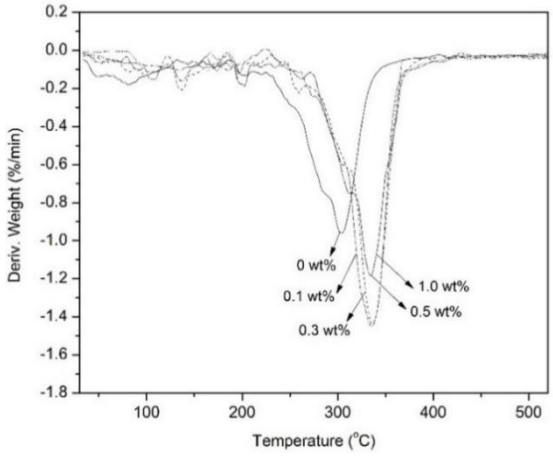

(b) Derivative weight curve.

Fig. 5. Thermal characteristic of nanocellulose loading in YB starch matrix.

4.6. Functional groups

Figure 6 shows FTIR results for the bionanocomposite. Troughs appear at wavenumber 3500-3000 cm^{-1} (-OH stretching), 2800-2900 cm^{-1} (C-H stretching) and 1600-1700 cm^{-1} (absorbed water groups) [3, 44, 45].

The wavenumber associated with functional groups of OH around 3000 cm^{-1} was reduced due to the formation of new hydrogen bonds between matrix and fiber [37, 46]. A similar result was reported by previous research who explain it in terms of weakened hydrogen bonding due to the delocalization of electrons [3, 44, 47]. The C-H stretching trough appeared at range wavenumber 2800-2900 cm^{-1} in all bionanocomposite samples indicating that they all contain aliphatic saturated components [48].

While the wavenumber of the -OH absorption water peak (1648 cm^{-1}) does not change, the transmittance of this peak increases steadily from 64.6% for pure YB starch film to 74.5%, for 1 wt% of reinforcing fiber indicating that water absorption is inversely proportional to the proportion of nanocellulose used [3, 49, 50].

4.7. Moisture absorption

Figure 7 shows the moisture absorption of all samples tested. YB starch with the addition of 0, 0.1, 0.3, 0.5, and 1 wt% nanocellulose suspension absorbs 19.1, 19.0, 18.7, 18.6 and 18.3% moisture respectively. Pure YB starch film is clearly more hydrophilic than the bionanocomposite films as the nanocellulose WHF forms a barrier preventing the water molecules from diffusing freely throughout the YB starch matrix [8, 37, 51]. Similar results have been reported by other researchers [21, 37, 50]. This result is supported by the FTIR transmittance data at wavenumber 1648 cm^{-1} (water absorption functional group) as discussed in the previous section.

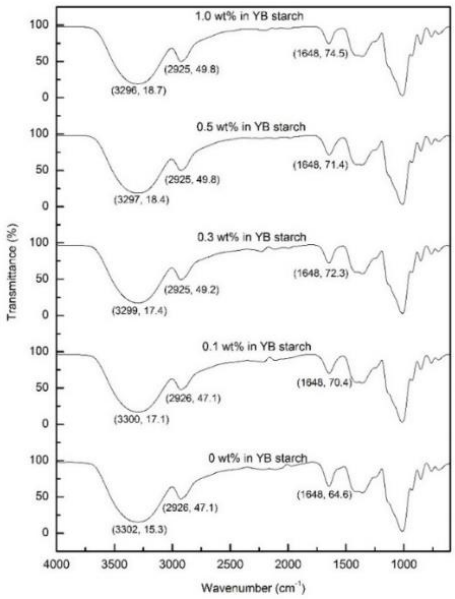

Fig. 6. FTIR of all bionanocomposite samples.

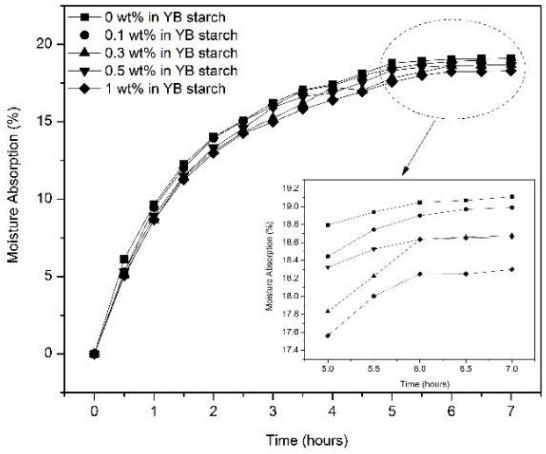

Fig. 7. Moisture absorption of all bionanocomposite samples.

5. Conclusions

Fabrication of bionanocomposites was successful through adding the nanocellulose in the form of a suspension in YB starch matrix followed by gelation and brief sonication. The addition of nanocellulose suspension in YB starch matrix given a brittle fracture formation of bionanocomposites. Sonication after gelation was also effective to disperse the nanocellulose homogeneously throughout the matrix as demonstrated by the measurements of mechanical properties. The maximum TS and TM were in the samples with the 1 wt% nanocellulose loading. This loading value improved tensile strength and resulted in good thermal stability, high crystallinity index, and decreased moisture absorption. The mechanical and thermal properties are comparable to that of plastics that are already being used for food packaging. The bionanocomposites are clear and manufactured from materials that are not only renewable but safe for human consumption. The addition of low amount nanocellulose fiber in YB starch matrix also resulting in significant improvement of their properties. Therefore, the potential of YB/WHF bionanocomposites could well be suitable for food packaging applications.

Acknowledgement

This research was funded by Directorate General of Higher Education Ministry of National Education, Indonesia, with the project name "Research of Master Program Leading to Doctoral Degree for Excellent Students (PMDSU)" Batch-2 in the year of 2018. We also thank Fay Farley for her proofreading.

Nomenclatures

CrI	Crystallinity index, %
H_a	Distance between baseline H_c with its baseline at (2θ=16.8^o)
H_c	Distance between maximum peak at (2θ=19.6^o) with baseline
I_{002}	The crystalline intensity at (2θ=22.6^o)
I_{am}	The amorphous intensity at (2θ=18^o)
W_o	Initial weight
W_t	Final weight

Greek Symbols

θ	Bragg angle, deg.
λ	Wavelength in XRD testing, nm

Abbreviations

DTG	Differential Thermal Gravimetry
EB	Elongation at Break
FTIR	Fourier Transform Infra-Red Spectroscopy
SEM	Scanning Electron Microscope
TEM	Transmission Electron Microscope
TGA	Thermogravimetric Analysis
TM	Tensile Modulus
TS	Tensile Strength
WHF	Water Hyacinth Fiber
XRD	X-ray Diffraction
YB	Yam Bean

References

1. Lendvai, L.; Karger-Kocsis, J.; Kmetty, A.; and Drakopoulos, S.X. (2016). Production and characterization of microfibrillated cellulose-reinforced thermoplastic starch composites. *Journal of Applied Polymer Science*, 133(2), 1-14.
2. Kaushik, A.; and Kaur, R. (2016). Thermoplastic starch nanocomposites reinforced with cellulose nanocrystals: Effect of plasticizer on properties. *Composite Interfaces*, 23(7), 701-717.
3. Kaewtatip, K.; and Thongmee, J. (2012). Studies on the structure and properties of thermoplastic starch/luffa fiber composites. *Materials and Design*, 40, 314-318.
4. Bootklad, M.; and Kaewtatip, K. (2013). Biodegradation of thermoplastic starch/eggshell powder composites. *Carbohydrate Polymers*, 97(2), 315-320.
5. Sanyang, M.L.; Sapuan, S.M.; Jawaid, M.; Ishak, M.R.; and Sahari, J. (2016). Effect of sugar palm-derived cellulose reinforcement on the mechanical and water barrier properties of sugar palm starch biocomposite films. *BioResources*, 11(2), 4134-4145.
6. Asrofi, M.; Abral, H.; Kasim, A.; and Pratoto, A. (2017). Characterization of the microfibrillated cellulose from water hyacinth pulp after alkali treatment and wet blending. *Proceedings of the 5th International Conference on Nanomaterials and Materials Engineering.* Bali, Indonesia, 7 pages.
7. Abral, H.; Kadriadi, D.; Rodianus, A.; Mastariyanto, P.; Ilhamdi; Arief, S.; Sapuan, S.M.; and Ishak, M.R. (2014). Mechanical properties of water hyacinth fibers-polyester composites before and after immersion in water. *Materials and Design*, 58, 125-129.
8. Asrofi, M.; Abral, H.; Kasim, A.; Pratoto, A.; Mahardika, M.; Park, J.W.; and Kim, H.J. (2018). Isolation of nanocellulose from water hyacinth fiber (WHF) produced via digester-sonication and its characterization. *Fibers and Polymers*, 19(8), 1618-1625
9. Asrofi, M.; Abral, H.; Kasim, A.; Pratoto, A.; Mahardika, M.; and Hafizulhaq, F. (2018). Mechanical properties of a water hyacinth nanofiber cellulose reinforced thermoplastic starch bionanocomposite: Effect of ultrasonic vibration during processing. *Fibers*, 6(40), 1-9
10. Teixeira, E. de M.; Pasquini, D.; Curvelo, A.A.S.; Corradini, E.; Belgacem, M.N.; and Dufresne, A. (2009). Cassava bagasse cellulose nanofibrils reinforced thermoplastic cassava starch. *Carbohydrate Polymers*, 78(3), 422-431.
11. Kargarzadeh, H.; Johar, N.; and Ahmad, I. (2017). Starch biocomposite film reinforced by multiscale rice husk fiber. *Composites Science and Technology*, 151, 147-155.
12. Abral, H.; Putra, G.J.; Asrofi, M.; Park, J.W.; and Kim, H.J. (2018). Effect of vibration duration of high ultrasound applied to bio-composite while gelatinized on its properties. *Ultrasonics Sonochemistry*, 40(Pt A), 697-702.
13. Gilfillan, W.N.; Moghaddam, L.; and Doherty, W.O.S. (2014). Preparation and characterization of composites from starch with sugarcane bagasse nanofibres. *Cellulose*, 21(4), 2695-2712.

14. Mahardika, M.; Abral, H.; Kasim, A.; Arief, S.; and Asrofi, M. (2018). Production of nanocellulose from pineapple leaf fibers via high-shear homogenization and ultrasonication. *Fibers*, 6(2), 1-12.
15. Wahono, S.; Irwan, A.; Syafri, E.; and Asrofi, M. (2018). Preparation and characterization of ramie cellulose nanofibers/$CaCO_3$ unsaturated polyester resin composites. *ARPN Journal of Engineering and Applied Sciences*, 13(2), 746-751.
16. Fu, Z.-q; Wu, M.; Han, X.-y; and Xu, L. (2017). Effect of okara dietary fiber on the properties of starch-baised films. *Starch-Starke*, 69(11-12), 7 pages.
17. Teixeira, E.D.M.; Lotti, C.; Correa, A.C.; Teodoro, K.B.; Marconcini, J.M.; and Mattoso, L.H. (2011). Thermoplastic corn starch reinforced with cotton cellulose nanofibers. *Journal of Applied Polymer Science*, 120(4), 2428-2433.
18. Asrofi, M.; Abral, H.; Putra, Y.K.; Sapuan, S.M.; and Kim, H.-J. (2018). Effect of duration of sonication during gelatinization on properties of tapioca starch water hyacinth fiber biocomposite. *International Journal of Biological Macromolecules*, 108, 167-176.
19. Abral, H.; Lawrensius, V.; Handayani, D.; and Sugiarti, E. (2018). Preparation of nano-sized particles from bacterial cellulose using ultrasonication and their characterization. *Carbohydrate Polymers*, 191(1), 161-167.
20. Agustin, M.B.; Ahmmad, B.; De Leon, E.R.P.; Buenaobra, J.L.; Salazar, J.R.; and Hirose, F. (2013). Starch-based biocomposite films reinforced with cellulose nanocrystals from garlic stalks. *Polymer Composites*, 34(8), 1325-1332.
21. Abdul Khalil, H.P.S.; Tye, Y.Y.; Saurabh, C.K.; Leh, C.P.; Lai, T.K.; Chong, E.W.N.; Fazita, M.R.N.; Hafiidz, J.M.; Banerjee, A.; and Syakir, M.I. (2017). Biodegradable polymer films from seaweed polysaccharides : A review on cellulose as a reinforcement material. *Express Polymer Letters*, 11(4), 244-265.
22. Soykeabkaew, N.; Laosat, N.; Ngaokla, A.; Yodsuwan, N.; and Tunkasiri, T. (2012). Reinforcing potential of micro- and nano-sized fibers in the starch-based biocomposites. *Composites Science and Technology*, 72(7), 845-852.
23. Nascimento, P.; Marim, R.; Carvalho, G.; and Mali, S. (2016). Nanocellulose produced from rice hulls and its effect on the properties of biodegradable starch films. *Materials Research*, 19(1), 167-174.
24. de Campos, A.; de Sena Neto, A.R.; Rodrigues, V.B.; Luchesi, B.R.; Moreira, F.K.V.; Correa, A.C.; Mattoso, L.H.C.; and Marconcini J.M. (2017). Bionanocomposites produced from cassava starch and oil palm mesocarp cellulose nanowhiskers. *Carbohydrate Polymers*, 175, 330-336.
25. Savadekar, N.R.; Karande, V.S.; Vigneshwaran, N.; Kadam, P.G.; and Mhaske, S.T. (2015). Preparation of cotton linter nanowhiskers by high-pressure homogenization process and its application in thermoplastic starch. *Applied Nanoscience*, 5(3), 281-290.
26. Cheng, W.; Chen, J.; Liu, D.; Ye, X.; and Ke, F. (2010). Impact of ultrasonic treatment on properties of starch film-forming dispersion and the resulting films. *Carbohydrate Polymers*, 81(3), 707-711.
27. Mali, S.; Grossmann, M.V.E.; Garcia, M.A.; Martino, M.N.; and Zaritzky, N.E. (2005). Mechanical and thermal properties of yam starch films. *Food Hydrocolloids*, 19(1), 157-164.

28. van Soest, J.J.; and Vliegenthart, J.FG. (1997). Crystallinity in starch plastics: Consequences for material properties. *Trends in Biotechnology*, 15(6), 208-213.
29. Abral, H.; Dalimunthe, M.H.; Hartono, J.; Efendi, R.P.; Asrofi, M.; Sugiarti, E.; Sapuan, S.M.; Park, J.-W.; and Kim, H.-J. Characterization of tapioca starch biopolymer composites reinforced with micro scale water hyacinth fibers. *Starch/Starke*, 70(7-8), 1700287.
30. Segal, L.; Creely, J.J.; Martin, A.E.; and Conrad, C.M. (1959). An empirical method for estimating the degree of crystallinity of native cellulose using the x-ray diffractometer. *Textile Research Journal*, 29(10), 786-794.
31. Hulleman, S.H.D.; Kalisvaart, M.G.; Janssen, F.H.P.; Feil, H.; and Vliegenthart, J.F.G. (1999). Origins of b-type crystallinity in glycerol-plasticized, compression-moulded potato starches. *Carbohydrate Polymers*, 39(4), 351-360.
32. Salaberria, A.M.; Diaz, R.H.; Labidi, J.; and Fernandes, S.C.M. (2015). Role of chitin nanocrystals and nanofibers on physical, mechanical and functional properties in thermoplastic starch films. *Food Hydrocolloids*, 46, 93-102.
33. Canigueral, N.; Vilaseca, F.; Mendez, J.A.; Lopez, J.P.; Barbera, L.; Puig, J.; Pelach, M.A.; and Mutje P. (2009). Behavior of biocomposite materials from flax strands and starch-based biopolymer. *Chemical Engineering Science*, 64(11), 2651-2658.
34. Nasution, H.; Harahap, H.; Afandy, Y.; and Al Fath, M.T. (2017). The Effect of cellulose nanocrystal (CNC) from rattan biomass as filler and citric acid as co-plasticizer on tensile properties of sago starch biocomposite. *Proceedings of the 3rd International on Applied Chemistry*. Jakarta, Indonesia, ID 120043.
35. Savadekar, N.R.; and Mhaske, S.T. (2012). Synthesis of nano cellulose fibers and effect on thermoplastics starch based films. *Carbohydrate Polymers*, 89(1), 146-151.
36. Karimi, S.; Tahir, P.M.; Dufresne, A.; Karimi, A.; and Abdulkhani, A. (2014). A comparative study on characteristics of nanocellulose reinforced thermoplastic starch biofilms prepared with different techniques. *Nordic Pulp & Paper Research Journal*, 29(1), 41-45.
37. Karimi, S.; Dufresne, A.; Md. Tahir, P.; Karimi, A.; and Abdulkhani, A. (2014). Biodegradable starch-based composites: Effect of micro and nanoreinforcements on composite properties. *Journal of Materials Science*, 49(13), 4513-4521.
38. Garcia, N.L.; Ribba, L.; Dufresne, A.; Aranguren, M.; and Goyanes, S. (2011). Effect of glycerol on the morphology of nanocomposites made from thermoplastic starch and starch nanocrystals. *Carbohydrate Polymers*, 84(1), 203-210.
39. Orue, A.; Corcuera, M.A.; Pena, C.; Eceiza, A.; and Arbelaiz, A. (2016). Bionanocomposites based on thermoplastic starch and cellulose nanofibers. *Journal of Thermoplastic Composite Materials*, 29(6), 817-832.
40. Prachayawarakorn, J.; Ruttanabus, P.; and Boonsom, P. (2011). Effect of cotton fiber contents and lengths on properties of thermoplastic starch composites prepared from rice and waxy rice starches. *Journal of Polymers and the Environment*, 19(1), 274-282.

41. Curvelo, A.A.S.; de Carvalho, A.J.F.; and Agnelli, J.A.M. (2001). Thermoplastic starch-cellulosic fibers composites: Preliminary results. *Carbohydrate Polymers*, 45(2), 183-188.
42. Awal, A.; Ghosh, S.B.; and Sain, M. (2010). Thermal properties and spectral characterization of wood pulp reinforced bio-composite fibers. *Journal of Thermal Analysis and Calorimetry*, 99(2), 695-701.
43. Lee, S.-Y.; Mohan, D.J.; Kang, I.-A.; Doh, G.-H.; Lee, S.; and Han, S.O. (2009). Nanocellulose reinforced PVA composite films: Effects of acid treatment and filler loading. *Fibers and Polymers*, 10(1), 77-82.
44. Cao, X.; Chen, Y.; Chang, P.R.; Muir, A.D.; and Falk, G. (2008). Starch-based nanocomposites reinforced with flax cellulose nanocrystals. *Express Polymer Letters*, 2(7), 502-510.
45. Asrofi, M.; Abral, H.; Kasim, A; and Pratoto, A. (2017). XRD and FTIR studies of nanocrystalline cellulose from water hyacinth (eichornia crassipes) fiber. *Journal of Metastable and Nanocrystalline Materials*, 29, 9-16.
46. Lubis, M.; Harahap, M.B.; Ginting, M.H.S.; Sartika, M.; and Azmi, H. (2018). Production of bioplastic from avocado seed starch reinforced with microcrystalline cellulose from sugar palm fibers. *Journal of Engineering Science and Technology* (*JESTEC*), 13(2), 381-393.
47. Prachayawarakorn, J.; Chaiwatyothin, S.; Mueangta S.; and Hanchana, A. (2013). Effect of jute and kapok fibers on properties of thermoplastic cassava starch composites. *Materials and Design*, 47, 309-315.
48. Lani, N.S.; Ngadi, N.; Johari, A.; and Jusoh, M. (2014). Isolation, characterization, and application of nanocellulose from oil palm empty fruit bunch fiber as nanocomposites. *Journal of Nanomaterials*, Article ID 702538, 10 pages.
49. Abral, H.; and Hartono, J. (2017). Moisture absorption of starch based biocomposites reinforced with water hyacinth fibers. *Proceedings of the Global Conference on Polymer and Composite Materials (PCM 2017*). Guangzhou, Guangdong, China, 5 pages.
50. Cyras, V.P.; Manfredi, L.B.; Ton-That, M.-T.; and Vazquez, A. (2008). Physical and mechanical properties of thermoplastic starch/montmorillonite nanocomposite films. *Carbohydrate Polymers*, 73(1), 55-63.
51. Balakrishnan, P.; Sreekala, M.S.; Kunaver, M.; Huskic, M.; and Thomas, S. (2017). Morphology, transport characteristics and viscoelastic polymer chain confinement in nanocomposites based on thermoplastic potato starch and cellulose nanofibers from pineapple leaf. *Carbohydrate Polymers*, 169, 176-188.